Bulk temperature and heat transport in turbulent Rayleigh–Bénard convection of fluids with temperature-dependent properties

Stephan Weiss[1], Xiaozhou He[1,2], Guenter Ahlers[1,3], Eberhard Bodenschatz[1,4,5] and Olga Shishkina[1],†

[1]Max Planck Institute for Dynamics and Self-Organization, Am Fassberg 17, 37077 Göttingen, Germany

[2]School of Mechanical Engineering and Automation, Harbin Institute of Technology, Shenzhen, China

[3]Department of Physics, University of California, Santa Barbara, CA 93106, USA

[4]Institute for Nonlinear Dynamics, Georg-August-University Göttingen, 37073 Göttingen, Germany

[5]Laboratory of Atomic and Solid-State Physics and Sibley School of Mechanical and Aerospace Engineering, Cornell University, Ithaca, NY 14853, USA

We critically analyse the different ways to evaluate the dependence of the Nusselt number (Nu) on the Rayleigh number (Ra) in measurements of the heat transport in turbulent Rayleigh–Bénard convection under general non-Oberbeck–Boussinesq conditions and show the sensitivity of this dependence to the choice of the reference temperature at which the fluid properties are evaluated. For the case when the fluid properties depend significantly on the temperature and any pressure dependence is insignificant we propose a method to estimate the centre temperature. The theoretical predictions show very good agreement with the Göttingen measurements by He *et al.* (*New J. Phys.*, vol. 14, 2012, 063030). We further show too the values of the normalized heat transport $Nu/Ra^{1/3}$ are independent of whether they are evaluated in the whole convection cell or in the lower or upper part of the cell if the correct reference temperatures are used.

Key words: Bénard convection, convection

1. Introduction

Natural thermal convection, which occurs in a fluid layer due to temperature differences, is omnipresent in nature and plays an important role in many engineering applications. A paradigm system to study this type of fluid motion is Rayleigh–Bénard convection (RBC), which takes place in a fluid layer confined between two horizontal plates, a lower heated plate and an upper cooled one (see, e.g. Bodenschatz, Pesch & Ahlers 2000; Ahlers, Grossmann & Lohse 2009; Lohse & Xia 2010; Chillà & Schumacher 2012).

Within the Oberbeck–Boussinesq (OB) approximation (Oberbeck 1879; Boussinesq 1903; Spiegel & Veronis 1960), all fluid properties are assumed to be pressure- and

† Email address for correspondence: Olga.Shishkina@ds.mpg.de

temperature independent, apart from the density in the buoyancy term, which is assumed to be a linear function of the temperature. Under the OB approximation, the RBC system is governed by the following dimensionless control parameters: the Rayleigh number Ra, the Prandtl number Pr and (for a cylindrical container) the diameter-to-height aspect ratio Γ:

$$Ra \equiv \frac{g\alpha\Delta H^3}{\nu\kappa}, \quad Pr \equiv \frac{\nu}{\kappa}, \quad \Gamma \equiv \frac{D}{H}. \quad (1.1a-c)$$

Here, $\Delta \equiv T_{bot} - T_{top}$ is the temperature difference between the hot bottom and cold top plates, H the height and D the diameter of the RBC cell, g the gravitational acceleration, ν the kinematic viscosity, κ the thermal diffusivity and α the isobaric thermal expansion.

In any real RBC experiment, however, the sample properties deviate from the OB approximation, since all material properties generally depend on the temperature and pressure. So-called non-Oberbeck–Boussinesq (NOB) effects become apparent, see Busse (1967), Gray & Giorgini (1976), Wu & Libchaber (1991), Zhang, Childress & Libchaber (1997), Niemela *et al.* (2000), Xia, Lam & Zhou (2002), Roche *et al.* (2004), Ahlers *et al.* (2006, 2007, 2008), Sugiyama *et al.* (2007), Sugiyama *et al.* (2009), Burnishev, Segre & Steinberg (2010), Horn, Shishkina & Wagner (2013), Horn & Shishkina (2014). The NOB effects influence the global flow structure and, therefore, can affect the global heat transport in the RBC system. This heat transport is usually expressed by the dimensionless Nusselt number, $Nu = q/\hat{q}$, that is, by the ratio of the total time averaged vertical heat flux q to the purely conductive heat flux $\hat{q}$.

While in many natural systems (e.g. in the atmosphere) large hydrostatic pressure differences cause variations of the fluid properties, the pressure variation across the fluid layer in laboratory RBC experiments is much smaller and the NOB effects are mainly caused by temperature variations. Even in the large-scale experiments in the 'Uboot' of Göttingen (Ahlers *et al.* 2012*b*; He *et al.* 2012), where pressurized sulfur hexafluoride (SF$_6$) is used in up to 2 m high RBC cells, the variations of the fluid properties with the temperature are at least 5 times larger than the variations of the fluid properties with the pressure. This is despite the large cell height and the fact that the density of SF$_6$ is approximately 5 times larger than the density of air. Also in large Ra-experiments with helium close to its critical point, the fluid property variations with the pressure are negligible compared to their strong variations with the temperature, see, e.g. Castaing *et al.* (1989), Ashkenazi & Steinberg (1999), Niemela & Sreenivasan (2003), Roche *et al.* (2004), Urban *et al.* (2014). Therefore, in the following we will focus on the NOB effects caused exclusively by temperature variations and assume a constant hydrostatic pressure throughout the cell.

Among the NOB effects, one of the most notable is a broken up–down symmetry of the convective flow and of the top and bottom boundary layers (BLs), as illustrated in figure 1. The broken symmetry results in a deviation of the centre temperature, T_c, from the arithmetic mean, $T_m \equiv (T_{top} + T_{bot})/2$, of the temperatures T_{top} and T_{bot} at the top and bottom plates, respectively.

Under NOB conditions, various questions arise, such as: What is the right way to calculate the Nusselt number Nu? How should Ra be calculated? In particular, at which reference temperature should the fluid properties be evaluated? Is it possible to deduce from the heat flux measurements under slightly NOB conditions the heat flux that would be measured in the OB case and which scaling relation of Nu versus Ra
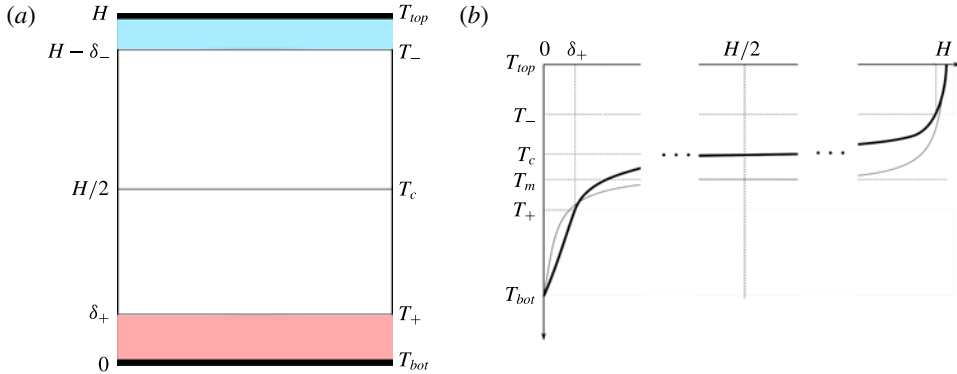
FIGURE 1. (Colour online) Sketch of a typical (*a*) NOB Rayleigh–Bénard convection cell and (*b*) mean vertical temperature profiles for a gas under NOB conditions (thick line) and a perfect OB fluid (thin line), as functions of the distance z from the heated bottom plate: the temperature at the bottom plate ($T = T_{bot}$ for $z = 0$), at the cross-over from the bottom BL to the bulk ($T = T_+$ for $z = \delta_+$), at mid-height of the cell ($T = T_c$ for $z = H/2$), at the cross-over from the top BL to the bulk ($T = T_-$ for $z = H - \delta_-$) and at the cooled top plate ($T = T_{top}$ for $z = H$). We have $T_{top} < T_- < T_c < T_+ < T_{bot}$ and $T_m \equiv (T_{bot} + T_{top})/2$. Pink and blue stripes correspond to the bottom and top BLs, respectively.

would be measured under perfect OB conditions? These questions became especially pertinent as different experiments, conducted at similar Ra, Pr and system geometries, have produced different scaling relations $Nu(Ra)$.

In previous work Shishkina, Weiss & Bodenschatz (2016) addressed the issue of how to calculate correctly the Nusselt number in measurements under general NOB conditions. There, an algorithm to calculate the mean conductive heat flux $\hat{q}$, which is needed for normalization of the measured total heat flux q, was presented.

Here we show the sensitivity of the Nu versus Ra relation to the reference temperatures at which the fluid properties are evaluated. For the case, when the fluid properties depend significantly on the temperature and any pressure dependence is unimportant, we propose a method to predict the centre temperature and show by example of the Göttingen measurements (Ahlers *et al.* 2012*b*; He *et al.* 2012) that it leads to more accurate predictions than the models based on an extension of the Prandtl–Blasius approach to a NOB case (Ahlers *et al.* 2006, 2007, 2008) or any of the three models by Wu & Libchaber (1991) or their modification (Urban *et al.* 2014).

In our approach we consider two virtual symmetric RBC cells I_- and I_+ filled with artificial fluids. The fluid properties are assumed to be functions of the temperature T that are symmetric about T_c. For I_- (I_+) they are taken to be equal to those of the real cell over the temperature range $T_{top} \leqslant T \leqslant T_c$ ($T_c \leqslant T \leqslant T_{bot}$).

We demonstrate that the Nu versus Ra scaling relations for the real cell and for both virtual cells are very similar. This means that it is impossible to remove the NOB effects in the Nu versus Ra relationship, while considering, for example, only the lower half of the real RBC cell. In particular, the transition, obtained in the measurements by Ahlers *et al.* (2012*b*) and He *et al.* (2012), is present in the scaling relations for the real cell as well as for the virtual symmetric cells, determined by the BLs like either the bottom BL or the top BL of the real RBC cell.

2. Model to predict the centre temperature in a real RBC cell

Here we develop a model to predict the temperature at mid-height, T_c, of a convection cell containing a fluid with properties that depend on the temperature. Hydrostatic pressure changes within the sample are assumed to be sufficiently small so that the dependence of the fluid properties on the pressure may be neglected.

In our model we assume that there are two BLs, one each adjacent to the top and bottom plate. The remainder of the system is regarded as the bulk. Thus we neglect the existence of mixing layers between the BLs and the bulk (see e.g. Kraichnan 1962; Chung, Yun & Adrian 1992), as well as the logarithmic profiles (Ahlers *et al.* 2012*a*; Ahlers, Bodenschatz & He 2014; Wei & Ahlers 2014) in the bulk just beyond the mixing layers. It turns out that this crude approximation is adequate for our purpose. We define two temperatures T_+ and T_- as the temperatures at suitably chosen locations of the cross-over from the BLs to the bulk. It also turns out that under the assumptions of the model the temperature drops across the BLs will not be needed. However, the model requires that fluid properties are evaluated at T_+ and T_-. We shall see below that these temperatures emerge naturally from the assumptions of the model (see (2.14)).

In figure 1 a typical mean vertical temperature profile is sketched, which has much larger temperature gradients within the BLs compared to that in the bulk region. Here T_+ and T_- are the temperatures at the cross-overs from the bottom and top thermal BLs to the bulk, respectively. The thicknesses of the bottom and top BLs are, respectively, δ_+ and δ_-. The drops of the temperature within the lower and upper halves of the convection cell,

$$\Delta_+ = T_{bot} - T_c, \quad \Delta_- = T_c - T_{top}, \quad (2.1a,b)$$

are generally different in a NOB case.

The absence of the top–bottom symmetry of the BLs in the real RBC cell causes a small deviation of the obtained Nusselt number (Nu) from that in the OB case. This deviation is small (except in the case of extreme deviations from the OB approximation) because, to lowest order, the effect on Nu from one of the BLs is nearly cancelled by an effect of similar magnitude but opposite sign from the other (see e.g. He, Bodenschatz & Ahlers 2016, §4). Here we address this small deviation, and perhaps more importantly the much larger shift of the centre temperature T_c away from the mean temperature T_m.

In our model we consider virtual symmetric RBC cells, filled with artificial fluids, the properties of which are symmetric (with respect to the central temperature T_c) functions of the temperature T. We will refer to these virtual systems as virtual symmetric RBC cells I_+ and I_-. The cells I_+ and I_- have *a priori* unknown heights H_+ and H_-, respectively. The bottom-plate temperature of the cell I_+ equals T_{bot} and the applied temperature difference is $2\Delta_+$. The top-plate temperature of the cell I_- equals T_{top} and the applied temperature difference is $2\Delta_-$. In each virtual cell, the temperature of the bottom plate is larger than the temperature of the top plate. The fluid properties of the cells I_- and I_+ are determined by the fluid properties of the real cell for the temperature ranges $T_{top} \leqslant T \leqslant T_c$ and $T_c \leqslant T \leqslant T_{bot}$, respectively. More precisely, for $T_{top} \leqslant T \leqslant T_c$, the fluid properties of the cell I_- are the same as those of the real cell, while for $T_c \leqslant T \leqslant T_{top} + 2\Delta_-$ the fluid properties of the cell I_- are obtained by reflection with respect to T_c. Analogously, for $T_c \leqslant T \leqslant T_{bot}$, the fluid properties of the cell I_+ are the same as those of the real cell, while for $T_{bot} - 2\Delta_+ \leqslant T \leqslant T_c$ the fluid properties of the cell I_+ are obtained by reflection with respect to T_c.

The total vertical heat flux averaged in time and over any horizontal cross-section in both cells, I_+ and I_-, is assumed to be equal to that in the real RBC cell, q. To calculate the Nusselt numbers for the corresponding cells,

$$Nu_+ \equiv q/\hat{q}_+ \quad \text{and} \quad Nu_- \equiv q/\hat{q}_-, \qquad (2.2a,b)$$

one needs the values of the mean vertical heat fluxes $\hat{q}_+$ and $\hat{q}_-$ that would occur via heat conduction alone, in the absence of convection, in the same cells. As the cells I_+ and I_- are symmetric, the conductive heat fluxes equal, respectively,

$$\hat{q}_+ = \lambda_+(2\Delta_+)/H_+ \quad \text{and} \quad \hat{q}_- = \lambda_-(2\Delta_-)/H_-. \qquad (2.3a,b)$$

Here $\lambda_\pm \equiv \lambda(T_\pm)$ is the thermal conductivity at the temperature $T_\pm$.

At this point it becomes necessary to decide upon which temperatures should be used to evaluate the conductivities λ_+ and λ_-, as well as the other fluid properties that will be needed below. Our definition of the virtual cells implies that the extrema of the properties will be at the plates (i.e. at T_{bot} or T_{top}) and at T_c. Thus we should choose a temperature somewhere between T_c and T_{bot} for I_+ and between T_{top} and T_c for I_-. Within our model we shall choose the cross-over temperatures T_+ and T_- for that purpose. While so far T_+ and T_- were defined only qualitatively, we shall see below that this choice will also lead to a unique definition of T_+ and T_-.

The Rayleigh numbers of the cells I_+ and I_- are, respectively,

$$Ra_+ = \eta_+(2\Delta_+)H_+^3 \quad \text{and} \quad Ra_- = \eta_-(2\Delta_-)H_-^3, \qquad (2.4a,b)$$

where $\eta_\pm \equiv \eta(T_\pm)$ and η is defined as $\eta \equiv \alpha g/(\kappa\nu)$.

Although the total vertical heat fluxes averaged in time and over any horizontal cross-section in both cells, I_+ and I_-, are equal to the same quantity, q, the Nusselt numbers and Rayleigh numbers of these symmetric cells can be different. However, we assume that the Nusselt numbers for both cells, although not equal to each other, follow the same scaling laws. That is,

$$Nu_+ = A_+ Pr_+^{a_+} Ra_+^{b_+} \quad \text{and} \quad Nu_- = A_- Pr_-^{a_-} Ra_-^{b_-} \qquad (2.5a,b)$$

with

$$A_+ = A_- = A, \quad a_+ = a_- = a \quad \text{and} \quad b_+ = b_- = b. \qquad (2.6a-c)$$

Here $Pr_\pm \equiv Pr(T_\pm) = \nu_\pm/\kappa_\pm$ is the Prandtl number evaluated at the temperature $T_\pm$. Note that this assumption is valid to a good approximation as long as (Pr_-, Ra_-) and (Pr_+, Ra_+) are sufficiently close, such that they belong to the same scaling regime, see Grossmann & Lohse (2000, 2001, 2004, 2011). Combining (2.2)–(2.6), we obtain:

$$\left(\frac{Nu_+}{Nu_-}\right)^{3b-1} \left(\frac{Pr_+}{Pr_-}\right)^a \left(\frac{\lambda_+}{\lambda_-}\right)^{3b} \left(\frac{\eta_+}{\eta_-}\right)^b \left(\frac{\Delta_+}{\Delta_-}\right)^{4b}. \qquad (2.7)$$

In the considered RBC experiments with SF_6, the Prandtl number is larger than 0.5 and, therefore, the scaling regimes there correspond to the 'upper' regimes in the Grossmann & Lohse (2000) theory. In the 'upper' regimes, $I_\infty^<$, III_∞ and IV_u in the terminology of Grossmann & Lohse (2000), the effective value of the scaling exponent

in the Nu versus Pr scaling relation is very close to zero, $a \approx 0$. Therefore, the Prandtl number dependence in the left-hand side of the relation (2.7) can be omitted:

$$\left(\frac{Nu_+}{Nu_-}\right)^{3-1/b} \left(\frac{\lambda_+}{\lambda_-}\right)^3 \left(\frac{\eta_+}{\eta_-}\right) \left(\frac{\Delta_+}{\Delta_-}\right)^4 = 1. \tag{2.8}$$

Furthermore, the effective value of the exponent b in the regimes $I_\infty^<$, III_∞ and IV_u is very close to 1/3 (see derivations for these regimes, respectively, in Grossmann & Lohse 2000, Grossmann & Lohse 2001 and Shishkina *et al.* 2017*a*). This means that the Nusselt number term in the left-hand side of the relation (2.8) can be also neglected as long as the Rayleigh number is not too high so that the so-called ultimate scaling of Nu versus Ra takes place. In the Göttingen experiments (Ahlers *et al.* 2012*b*; He *et al.* 2012) for high Ra, where already a transition to the ultimate regime takes place, the effective value of b is approximately 0.38, but even in this case the variation of the Nusselt number, taken to the power $(3 - 1/b)$, is much smaller than the variation of the fluid properties. Indeed, even if the Nusselt number variation would be as large as 40 % ($Nu_-/Nu_+ = 1.4$), the variation of the Nusselt number term in the relation (2.8) is only approximately 12 % ($(Nu_+/Nu_-)^{3-1/b} \approx 0.88$), while η has a much stronger variation. For example, in the experiments by Ahlers *et al.* (2012*b*) and He *et al.* (2012) with SF_6, it can be up to 300 % larger close to the cold plate than near the warm plate. The λ-term in the relation (2.8) also cannot be neglected, however, the λ-variation of SF_6 is not as large as the η-variation. Note that the above considered 40 % variation of the Nusselt number occurs not from the measurements by Ahlers *et al.* (2012*b*) and He *et al.* (2012), but is just taken as a very upper bound.

Thus, with the above explanations, we obtain from the relation (2.8) the following temperature balance relation:

$$\lambda_+^3 \eta_+ \Delta_+^4 \approx \lambda_-^3 \eta_- \Delta_-^4, \tag{2.9}$$

where the fluid properties $\lambda_\pm$ and $\eta_\pm$ are evaluated at the temperature $T_\pm$. Equation (2.9) is equivalent to

$$T_c = \frac{\lambda_+^{3/4} \eta_+^{1/4} T_{bot} + \lambda_-^{3/4} \eta_-^{1/4} T_{top}}{\lambda_+^{3/4} \eta_+^{1/4} + \lambda_-^{3/4} \eta_-^{1/4}}. \tag{2.10}$$

As T_+ and T_- correspond to the temperatures at the cross-overs from the corresponding BLs to the bulk of the real cell, we shall represent them as a linear combination of the centre temperature and the temperature of the corresponding plate, as follows:

$$T_+ = \beta_+ T_{bot} + (1 - \beta_+) T_c, \tag{2.11}$$

$$T_- = \beta_- T_{top} + (1 - \beta_-) T_c. \tag{2.12}$$

Although the temperature gradients in the BLs of a real RBC cell are very steep, the BLs are not purely conductive but are highly fluctuating for sufficiently large Ra, see, e.g. du Puits *et al.* (2007), du Puits, Resagk & Thess (2013). For a fixed aspect ratio of the container, the mean temperature profiles within the BLs depend slightly on Pr and very weakly on Ra, see Shishkina *et al.* (2015, 2017*b*) and Ching, Dung & Shishkina (2017). Therefore, in a fully developed turbulent RBC flow, the temperature

at the BL–bulk cross-over depends on Pr, although quite weakly. Based on this and the fact that $Pr_+ \approx Pr_-$, we assume further that

$$\beta_+ = \beta_- = \beta \qquad (2.13)$$

for a certain value of β, $0 \leqslant \beta \leqslant 1$. Thus, we write

$$\left. \begin{aligned} T_+ &= \beta T_{bot} + (1 - \beta)T_c, \\ T_- &= \beta T_{top} + (1 - \beta)T_c. \end{aligned} \right\} \qquad (2.14)$$

Relations (2.10), (2.14) build a model to predict the bulk, or central, temperature T_c in the real RBC cells. Note that although (2.10) is nonlinear, its numerical solution can be obtained quite easily, using an iterative procedure, as soon as the value of β in (2.14) is known.

As one can see in figure 2, the model (2.10) is very sensitive to the accuracy of the approximation of β in the relations (2.14). In figure 2 the estimates of the relative temperature deviations, $(T_m - T_c)/\Delta$, in pressurized gas SF_6 are presented, according to (2.10), (2.14), for different values of β_{appr} in the approximation $\beta \approx \beta_{appr}$. The case $\beta_{appr} = 0$ would propose that the temperature at the cross-over from the BL to the bulk equals the centre temperature, $T_\pm = T_c$, and the case $\beta_{appr} = 1$ would mean that at the cross-over from the BL to the bulk the temperature equals the plate temperature. Because of the strong sensitivity of the model (2.10) on the quality of the approximation of β, it is extremely important to estimate the value of β possibly precise.

The value of β is strongly influenced by the geometry of the container, which is determined mainly by its diameter-to-height aspect ratio Γ. In slender containers, when Γ is small, the temperature gradient in the bulk is not negligible and, therefore, β is relatively large. For large Γ and sufficiently large Ra, the mean temperature gradient vanishes in the bulk and, therefore, β is relatively small. When Γ tends to infinity, the value of β saturates at a certain fixed value β_0, which generally depends on Pr and Ra. Assuming an exponential dependence of β on Γ, we approximate β with $\beta_{\text{Gö}}$, where

$$\beta \approx \beta_{\text{Gö}} = (1 - \beta_0) \exp(-B\Gamma) + \beta_0. \qquad (2.15)$$

The coefficient B, $B > 0$, which generally depends on Pr and Ra, shows how fast β saturates at β_0 when $\Gamma \to \infty$.

From an analysis of the mean temperatures at the cross-overs from the BLs to the bulk in RBC for different Ra and Pr but fixed Γ, one can conclude that this temperature and, hence, also the value of β are influenced by Pr and depend negligibly weak on Ra, as soon as the convective flow is turbulent (Shishkina *et al.* 2017*b*). The value of β_0 is slightly larger for smaller Pr, larger Ra and near the lateral walls, where stronger fluctuations are observed. For $Pr \approx 1$ it can be estimated from the solution of the thermal boundary layer equation that takes into account the turbulent fluctuations in terms of the eddy thermal diffusivity (Shishkina *et al.* 2015). In this case, the vertical profile of the dimensionless temperature θ, which is equal to 0 at the plate ($\xi = 0$) and equals 1 in the bulk ($\xi \to \infty$), is described by the following analytical expression:

$$\theta(\xi) = \frac{\sqrt{3}}{4\pi} \log \frac{(1 + e\xi)^3}{1 + (e\xi)^3} + \frac{3}{2\pi} \arctan \frac{2e\xi - 1}{\sqrt{3}} + \frac{1}{4} \qquad (2.16)$$
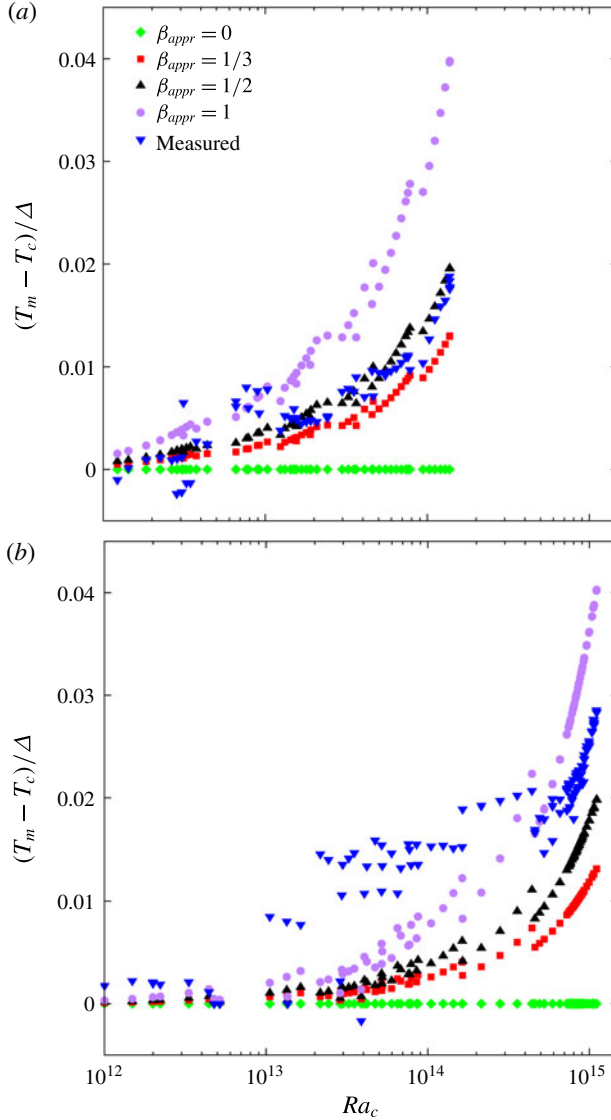
FIGURE 2. (Colour online) Sensitivity of the model (2.10) to the accuracy of the approximation of $\beta \approx \beta_{appr}$ in the relations (2.14). Shown are predictions for different values of β_{appr} against the measurements in pressurized SF_6, for the cell aspect ratios (a) $\Gamma = 1$ (He *et al.* 2012) and (b) $\Gamma = 1/2$ (Ahlers *et al.* 2012b). The predicted or measured values of the relative deviation of T_c from T_m are plotted against the Rayleigh number evaluated at the measured T_c.

with $e = 2\pi/(3\sqrt{3})$. Here ξ is the dimensionless distance from the plate, where $\xi = 1$ corresponds to the cross-over from the BL to the bulk. Since $\theta(1) \approx 0.765$, we obtain that for $Pr \approx 1$ the value of β_0 equals $\beta_0 = 1 - \theta(1) \approx 0.235$. We cannot derive the value of B in (2.15) from the BL equations and, therefore, fit it from the available experimental data. Thus, we complement the relation (2.15) with

$$\beta_0 = 0.235 \quad \text{and} \quad B = 1.14. \tag{2.17a,b}$$

Any choice of B within the interval [1.1; 1.2] would not change much the predictions of the central temperature. Thus, for the largest studied Ra we obtained that the relative deviation of the predictions for $B = 1.2$ and $B = 1.1$ is less than 0.07 %. Although the values of B and β_0 defined by (2.17) are only rough approximations, they, together with (2.10)–(2.15), lead to quite accurate predictions of the centre temperature in the cases considered in the next section. In the future, the estimates (2.17) of β_0 and B will be eventually updated and formulated as Pr- and Ra-dependences. For more accurate estimates one needs more measurements of the centre temperature, for possibly high Ra and different values of Γ and Pr.

3. Comparison with other models

Now we compare the proposed model (2.10)–(2.17) with other existing models and measurements.

In Horn *et al.* (2013), Horn & Shishkina (2014), models to predict the centre temperature T_c in RBC, including those by Wu & Libchaber (1991), Zhang *et al.* (1997), Manga & Weeraratne (1999), Ahlers *et al.* (2006), were compared, based on direct numerical simulations. For the case of very strong temperature dependence of the fluid properties, the models by Wu & Libchaber (1991) (more precisely, their second and third model) were more accurate than the other models. Therefore in the present work we restrict our consideration to the model by Ahlers *et al.* (2007, 2008) and the three models by Wu & Libchaber (1991) and a slight modification of their first model by Urban *et al.* (2014) and compare them with our model (2.10)–(2.17) to predict the centre temperature T_c, which was proposed in the previous section.

Let us first recollect the models by Wu & Libchaber (1991). There, the following rough approximations are used: the total temperature drop is assumed to take place exclusively across the bottom and top BLs and heat is assumed to be transported purely by conduction within the BLs, i.e. $q = \lambda_b \Delta_+ / \delta_+ = \lambda_t \Delta_- / \delta_-$. The reference temperature T_b (T_t) of the bottom (top) BL, at which the corresponding values of the fluid properties λ_b and η_b (λ_t and η_t) are evaluated, is defined as follows:

$$T_b \equiv (T_{bot} + T_c)/2, \quad \text{and} \quad T_t \equiv (T_{top} + T_c)/2. \quad (3.1a,b)$$

To close the system of the above equations, Wu & Libchaber (1991), in their first model, follow Malkus (1954) and Howard (1966) and assume that the Rayleigh numbers for the BLs are equal, i.e. $\eta_b \Delta_+ \delta_+^3 = \eta_t \Delta_- \delta_-^3$. This leads to their first model:

$$\lambda_b^3 \eta_b \Delta_+^4 = \lambda_t^3 \eta_t \Delta_-^4. \quad (3.2)$$

One can see that this model coincides with our model (2.10) if, instead of (2.15), the value $\beta = 1/2$ is taken in the relations (2.14).

Following Castaing *et al.* (1989), in the second model by Wu & Libchaber (1991), it is assumed that the reference velocities w_b and w_t of the thermal plumes emitted from the two BLs are similar, $w_b \approx w_t$. The reference plume velocity w_b (w_t) of the bottom (top) BL is estimated by the balance of the buoyancy force and the viscous force, i.e. $g\alpha_b \Delta_+ = \nu_b w_b / \delta_+^2$ ($g\alpha_t \Delta_- = \nu_t w_t / \delta_-^2$). This leads to their second model:

$$\lambda_b^2 \eta_b \kappa_b \Delta_+^3 = \lambda_t^2 \eta_t \kappa_t \Delta_-^3. \quad (3.3)$$

In the third model by Wu & Libchaber (1991), it is assumed that the inversed temperature scales of the BLs are similar, i.e. $\eta_b \delta_+^3 = \eta_t \delta_-^3$, which leads to the following relation:

$$\lambda_b^3 \eta_b \Delta_+^3 = \lambda_t^3 \eta_t \Delta_-^3. \quad (3.4)$$

To estimate the centre temperature T_c with the models by Wu & Libchaber (1991), one needs to solve the corresponding nonlinear equations (3.2)–(3.4). A modification of their first model (3.2) was also considered by Urban *et al.* (2014), where instead of (3.1), the following approximations of the reference temperatures of the BLs were used:

$$T_b \equiv (T_{bot} + T_m)/2 = (3T_{bot} + T_{top})/4, \left.\right\} \\ T_t \equiv (T_{top} + T_m)/2 = (T_{bot} + 3T_{top})/4. \left.\right\} \tag{3.5}$$

This modification allowed for estimation of T_c using the explicit relations (3.2), (3.5).

The last model, which we compare our model with, is an extension of the Prandtl–Blasius BL theory to a general NOB case of compressible flows, which was developed by Ahlers *et al.* (2006, 2007, 2008). There, the centre temperature is found based on an assumption of asymmetric BLs, which, however, follow the Prandtl–Blasius BL equations. Since the temperature profiles in Oberbeck–Boussinesq RBC deviate significantly from the Prandtl–Blasius predictions, the extension of the Prandtl–Blasius BL theory to a non-Oberbeck–Boussinesq case inherits similar problems (see, e.g. Ahlers *et al.* 2008, figure 11). This limits the applicability of the extended Prandtl–Blasius BL theory to predict the centre temperature in NOB RBC. Note that the deviations between the predictions of the Prandtl–Blasius BL theory and real temperature profiles are larger for larger *Ra* and smaller *Pr*, see theoretical explanations in Shishkina *et al.* (2015, 2017b) and Ching *et al.* (2017), and results of direct numerical simulations in, e.g. Scheel, Kim & White (2012), Stevens *et al.* (2012), Shishkina, Horn & Wagner (2013), Shishkina, Wagner & Horn (2014).

In figure 3 we compare our model (2.10)–(2.17) with the model by Ahlers *et al.* (2007, 2008) and with the three models (3.2)–(3.4), (3.1) by Wu & Libchaber (1991) and a modification of their first model (3.2), (3.5). The comparison is made using the measurements of the bulk temperature in the RBC experiments with pressurized SF$_6$ in cylindrical containers of the diameter-to-height aspect ratios $\Gamma = 1$ (He *et al.* 2012) and $\Gamma = 1/2$ (Ahlers *et al.* 2012b).

For the case $\Gamma = 1$ (figure 3a), the predictions of our model (2.10)–(2.17) are in perfect agreement with the measurements by He *et al.* (2012) and the proposed model excels all other considered models. The third model by Wu & Libchaber (1991) significantly overestimates the relative deviation of the centre temperature from the arithmetic mean of the top and bottom temperatures, while the model by Ahlers *et al.* (2007, 2008) underestimates it.

In the case $\Gamma = 1/2$ (figure 3b), for the highest *Ra*, where the measurements of the temperature deviation are most precise, the predictions of our model (2.10)–(2.17) are again in good agreement with the measurements. In this case, in contrast to what was obtained for $\Gamma = 1$, the predictions of the first and second models by Wu & Libchaber (1991) underestimate the temperature deviation; so does the model by Ahlers *et al.* (2007, 2008).

4. Comments on the scaling relations of the compensated Nusselt number with the Rayleigh number

In the previous sections, for the purpose of estimating the centre temperature in a real RBC cell, we considered two virtual symmetric RBC cells, $I_{\pm}$, which can be understood as an approximation of the real RBC cell. This approximation is the next closest to the OB approximation, which takes into account the temperature variation of the fluid properties.
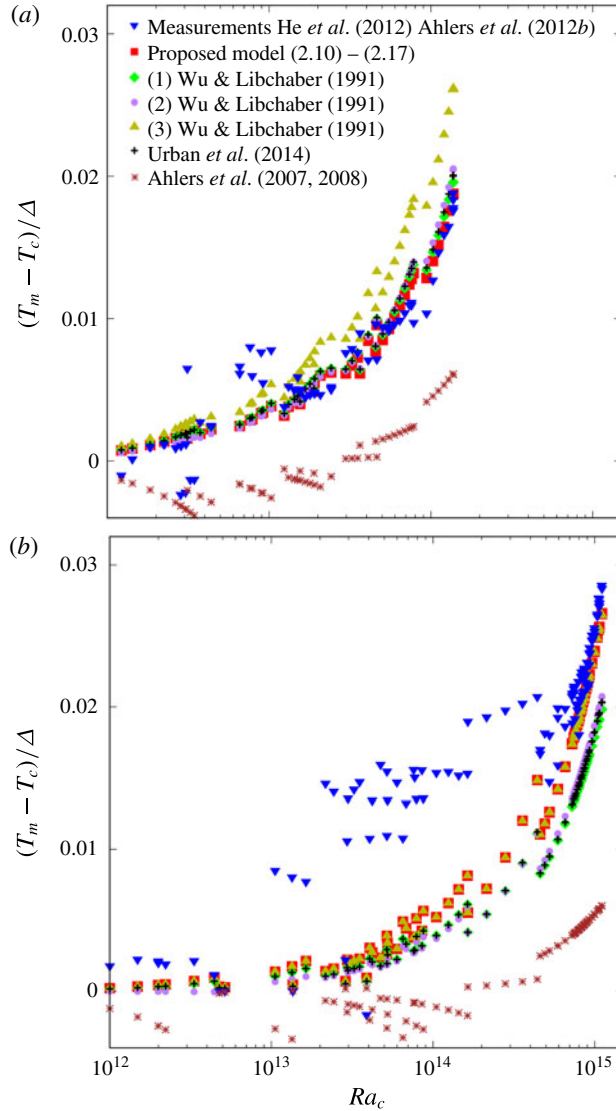
FIGURE 3. (Colour online) Comparison of the measured relative deviation of the centre temperature from the arithmetic mean of the top and bottom temperatures in the RBC experiments with pressurized SF_6 by (*a*) He *et al.* (2012), for the aspect ratio $\Gamma = 1$ and by (*b*) Ahlers *et al.* (2012*b*), for $\Gamma = 1/2$, with the predictions of the here proposed model (2.10)–(2.17) and earlier models by Ahlers *et al.* (2007, 2008), three models by Wu & Libchaber (1991) and a modification of their first model by Urban *et al.* (2014).

Although the virtual symmetric cells $I_\pm$ and the real RBC cell can generally have different heights, $H_\pm$ and H, respectively, the compensated Nusselt numbers,

$$\frac{Nu_+}{Ra_+^{1/3}} = \frac{q}{\lambda(T_+)[16(T_{bot} - T_c)^4 \eta(T_+)]^{1/3}}, \tag{4.1}$$

$$\frac{Nu_-}{Ra_-^{1/3}} = \frac{q}{\lambda(T_-)[16(T_c - T_{top})^4 \eta(T_-)]^{1/3}} \tag{4.2}$$

are independent of the heights. The Nusselt numbers here are assumed to be calculated according to the definition, as proposed in Shishkina *et al.* (2016). Obviously, in the OB case, the values of $Nu_\pm/Ra_\pm^{1/3}$ and $Nu/Ra_c^{1/3}$ coincide. How different are $Nu_\pm/Ra_\pm^{1/3}$ and $Nu/Ra_c^{1/3}$ under NOB conditions, with the temperature-dependent fluid properties?

When the exact values of the temperatures at the cross-overs from the BLs to the bulk, $T_\pm$, and the centre temperature T_c are known, the fluid properties $\eta_\pm$ and $\lambda_\pm$ at these temperatures and, hence, the compensated Nusselt numbers $Nu_\pm/Ra_\pm^{1/3}$ can be easily calculated. In the case, when T_c is known, but $T_\pm$ is not known, one can use the approximation (2.14)–(2.17), to estimate $T_\pm$. In most measurements of the mean heat transport in RBC, not only $T_\pm$, but also T_c is not available. In such cases the model (2.10)–(2.17) can be used to estimate T_c and $T_\pm$.

As discussed above, inaccurate approximations of β in the relations (2.14) lead to inaccurate predictions of the bulk temperature T_c (see, for example, figure 2 for $\beta \approx \beta_{appr}$ with different values of β_{appr}), while an accurate approximation $\beta_{appr} = \beta_{G\ddot{o}}$, according to (2.15) and (2.17), leads to precise predictions of T_c (see figure 3).

In figures 4 and 5, the dependences of the compensated Nusselt numbers, i.e. $Nu_\pm/Ra_\pm^{1/3}$ against the measured Rayleigh numbers Ra_c are presented for the virtual symmetric RBC cells $I_\pm$, by example of the RBC data for pressurized SF_6. The cases $\Gamma = 1$ and $\Gamma = 1/2$ are presented, respectively, in figures 4 and 5. There $Nu_\pm/Ra_\pm^{1/3}$ calculated for different reference temperatures $T_\pm$ (i.e. different approximations of β), are plotted against Ra_c. For an inaccurate approximation $\beta \approx \beta_{appr}$ with $\beta_{appr} = 0$ (when the temperature at the cross-over from the BL to the bulk is assumed to be equal to the centre temperature), the dependence $Nu_+/Ra_+^{1/3}$ on the Rayleigh number is decreasing, while $Nu_-/Ra_-^{1/3}$ is increasing (see figures 4a and 5a). Opposite to this, for another inaccurate approximation, i.e. $\beta_{appr} = 1$ (when the temperature at the cross-over from the BL to the bulk is assumed to be equal to the temperature at the corresponding plate), the dependence $Nu_+/Ra_+^{1/3}$ on the Rayleigh number is increasing, while $Nu_-/Ra_-^{1/3}$ is decreasing (see figures 4c and 5c).

With an accurate approximation $\beta_{appr} = \beta_{G\ddot{o}}$ (which leads to the correct values of the centre temperature T_c and of the temperatures at the cross-overs from the BLs to the bulk, $T_\pm$, see (2.15), (2.17)), the scalings relations of $Nu_\pm/Ra_\pm^{1/3}$ versus Ra_c and $Nu/Ra_c^{1/3}$ versus Ra_c are very similar. One can see this in figure 4(b) for $\Gamma = 1$ and figure 5(b) for $\Gamma = 1/2$. These three scaling relations almost replicate each other and, in particular, the transition (i.e. an increase of the normalized Nusselt numbers for large Ra), reported in Ahlers *et al.* (2012b), He *et al.* (2012) is visible not only in the $Nu/Ra_c^{1/3}$ dependence, but also in the $Nu_+/Ra_+^{1/3}$ and $Nu_-/Ra_-^{1/3}$ dependences. Note that plotting $Nu_\pm/Ra_\pm^{1/3}$ versus $Ra_\pm$ instead of $Nu_\pm/Ra_\pm^{1/3}$ versus Ra_c would only stretch or compress the plots in the horizontal direction, and therefore will not affect the presence of the transition.

5. Conclusions

In the present work we use a thought experiment introducing two virtual cells, as described in § 2, to derive a model (2.10)–(2.17) for non-Oberbeck–Boussinesq thermal convection, where the fluid properties depend exclusively on the temperature and are almost independent of the pressure. We show that the model with quantifiable assumptions allows to estimate the centre temperature T_c in turbulent RBC, according
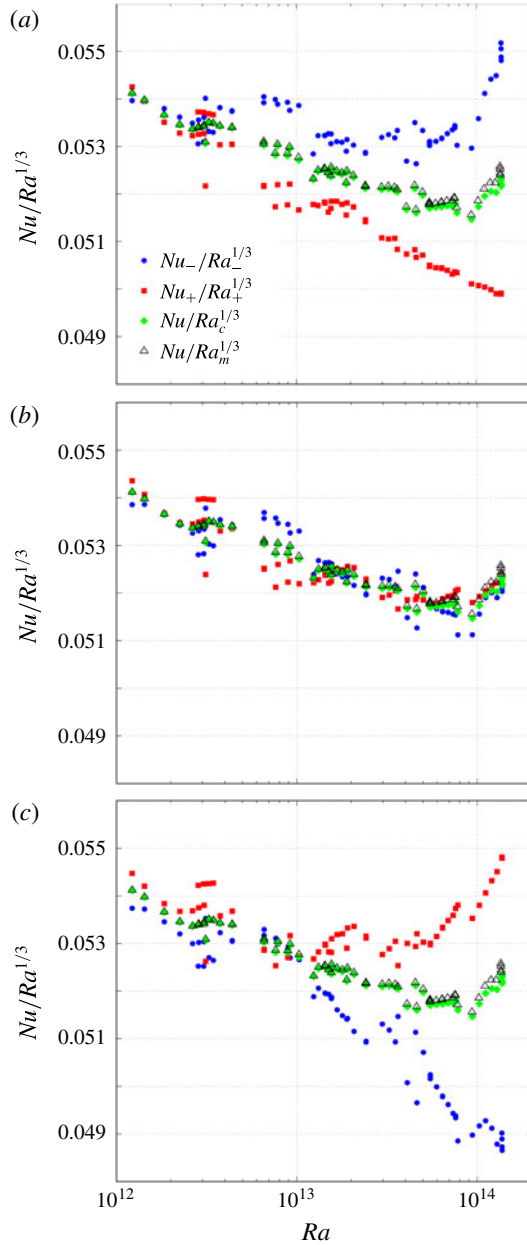
FIGURE 4. (Colour online) Sensitivity of the dependences $Nu_{\pm}/Ra_{\pm}^{1/3}$ versus Ra_c to the temperatures $T_{\pm}$ at which the fluid properties are evaluated (obtained using an approximation $\beta \approx \beta_{appr}$ in (2.14)), for virtual symmetric RBC cells with the BLs like the warm BL (squares) or like the cold BL (circles) in a real RBC cell, by example of the measurements by He *et al.* (2012) for $\Gamma = 1$. The values of $Nu_{\pm}/Ra_{\pm}^{1/3}$ are evaluated according to (4.1), (4.2), for measured T_c and (a,c) inaccurate approximations (a) $\beta_{appr} = 0$ and (c) $\beta_{appr} = 1$ and (b) an accurate approximation $\beta_{appr} = \beta_{G\ddot{o}}$, according to (2.15), (2.17). The dependences $Nu/Ra_m^{1/3}$ versus Ra_m (triangles) and $Nu/Ra_c^{1/3}$ versus Ra_c (diamonds) are shown for comparison.
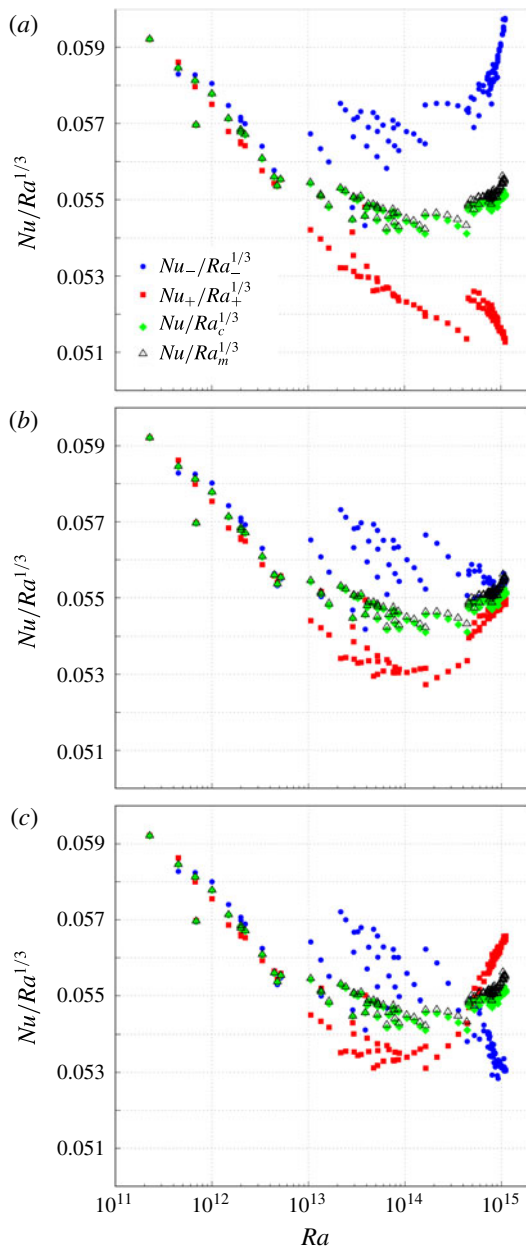
FIGURE 5. (Colour online) Sensitivity of the dependences $Nu_\pm/Ra_\pm^{1/3}$ versus Ra_c to the temperatures $T_\pm$ at which the fluid properties are evaluated (obtained using an approximation $\beta \approx \beta_{appr}$ in (2.14)), for virtual symmetric RBC cells with the BLs like the warm BL (squares) or like the cold BL (circles) in a real RBC cell, by example of the measurements by Ahlers *et al.* (2012*b*) for $\Gamma = 1/2$. The values of $Nu_\pm/Ra_\pm^{1/3}$ are evaluated according to (4.1), (4.2), for measured T_c and (*a,c*) inaccurate approximations (*a*) $\beta_{appr} = 0$ and (*c*) $\beta_{appr} = 1$ and (*b*) an accurate approximation $\beta_{appr} = \beta_{Gö}$, according to (2.15), (2.17). The dependences $Nu/Ra_m^{1/3}$ versus Ra_m (triangles) and $Nu/Ra_c^{1/3}$ versus Ra_c (diamonds) are shown for comparison.

to (2.10). The fluid properties in (2.10) are evaluated at the temperatures $T_{\pm}$, see (2.14), where the parameter β is approximated according to the relations (2.15), (2.17).

The model admits that the Rayleigh numbers of the top and bottom BLs can be different, but the scaling laws of the Nusselt number versus the Prandtl number and Rayleigh number are the same. Based on the measurements by Ahlers *et al.* (2012*b*) and He *et al.* (2012) in containers of the aspect ratios $\Gamma = 1$ and $\Gamma = 1/2$, we showed that the model leads to very precise estimates of T_c in turbulent NOB RBC.

Finally, based on the above measurements, we showed that the compensated values of the heat transport, i.e. $Nu/Ra^{1/3}$, evaluated for the real RBC cell with the reference temperature T_c or for the virtual symmetric RBC cell, with the BLs like the bottom or top BL in the real cell, are very similar if the correct reference temperatures T_+ and T_- are considered for these symmetric cells.

Acknowledgements

REFERENCES

AHLERS, G., ARAUJO, F. F., FUNFSCHILLING, D., GROSSMANN, S. & LOHSE, D. 2007 Non-Oberbeck–Boussinesq effects in gaseous Rayleigh–Bénard convection. *Phys. Rev. Lett.* **98**, 054501.

AHLERS, G., BODENSCHATZ, E., FUNFSCHILLING, D., GROSSMANN, S., HE, X., LOHSE, D., STEVENS, R. J. A. M. & VERZICCO, R. 2012*a* Logarithmic temperature profiles in turbulent Rayleigh–Bénard convection. *Phys. Rev. Lett.* **109**, 114501.

AHLERS, G., BODENSCHATZ, E. & HE, X. 2014 Logarithmic temperature profiles of turbulent Rayleigh–Bénard convection in the classical and ultimate state for a Prandtl number of 0.8. *J. Fluid Mech.* **758**, 436–467.

AHLERS, G., BROWN, E., ARAUJO, F. F., FUNFSCHILLING, D., GROSSMANN, S. & LOHSE, D. 2006 Non-Oberbeck–Boussinesq effects in strongly turbulent Rayleigh–Bénard convection. *J. Fluid Mech.* **569**, 409–446.

AHLERS, G., CALZAVARINI, E., ARAUJO, F. F., FUNFSCHILLING, D., GROSSMANN, S., LOHSE, D. & SUGIYAMA, K. 2008 Non-Oberbeck–Boussinesq effects in turbulent thermal convection in ethane close to the critical point. *Phys. Rev.* E **77**, 046302.

AHLERS, G., GROSSMANN, S. & LOHSE, D. 2009 Heat transfer and large scale dynamics in turbulent Rayleigh–Bénard convection. *Rev. Mod. Phys.* **81**, 503–537.

AHLERS, G., HE, X., FUNFSCHILLING, D. & BODENSCHATZ, E. 2012*b* Heat transport by turbulent Rayleigh–Bénard convection for $Pr \simeq 0.8$ and $3 \times 10^{12} \lesssim Ra \lesssim 10^{15}$: aspect ratio $\Gamma = 0.50$. *New J. Phys.* **14**, 103012.

ASHKENAZI, S. & STEINBERG, V. 1999 High Rayleigh number turbulent convection in a gas near the gas–liquid critical point. *Phys. Rev. Lett.* **83**, 3641–3644.

BODENSCHATZ, E., PESCH, W. & AHLERS, G. 2000 Recent developments in Rayleigh–Bénard convection. *Annu. Rev. Fluid Mech.* **32**, 709–778.

BOUSSINESQ, J. 1903 *Théorie Analytique de la Chaleur*. Gauthier-Villars.

BURNISHEV, Y., SEGRE, E. & STEINBERG, V. 2010 Strong symmetrical non-Oberbeck–Boussinesq turbulent convection and the role of compressibility. *Phys. Fluids* **22**, 035108.

BUSSE, F. H. 1967 The stability of finite amplitude cellular convection and its relation to an extremum principle. *J. Fluid Mech.* **30**, 625–649.

CASTAING, B., GUNARATNE, G., HESLOT, F., KADANOFF, L., LIBCHABER, A., THOMAE, S., WU, X.-Z., ZALESKI, S. & ZANETTI, G. 1989 Scaling of hard thermal turbulence in Rayleigh–Bénard convection. *J. Fluid Mech.* **204**, 1–30.

CHILLÀ, F. & SCHUMACHER, J. 2012 New perspectives in turbulent Rayleigh–Bénard convection. *Eur. Phys. J.* E **35**, 58.

CHING, E. S. C., DUNG, O.-Y. & SHISHKINA, O. 2017 Fluctuating thermal boundary layers and heat transfer in turbulent Rayleigh–Bénard convection. *J. Stat. Phys.* **167**, 626–635.

CHUNG, M. K., YUN, H. C. & ADRIAN, R. J. 1992 Scale analysis and wall-layer model for the temperature profile in a turbulent thermal convection. *Intl J. Heat Mass Transfer* **35**, 43–51.

GRAY, D. D. & GIORGINI, A. 1976 The validity of the Boussinesq approximation for liquids and gases. *Intl J. Heat Mass Transfer* **19**, 545–551.

GROSSMANN, S. & LOHSE, D. 2000 Scaling in thermal convection: a unifying theory. *J. Fluid Mech.* **407**, 27–56.

GROSSMANN, S. & LOHSE, D. 2001 Thermal convection for large Prandtl numbers. *Phys. Rev. Lett.* **86**, 3316–3319.

GROSSMANN, S. & LOHSE, D. 2004 Fluctuations in turbulent Rayleigh–Bénard convection: the role of plumes. *Phys. Fluids* **16**, 4462–4472.

GROSSMANN, S. & LOHSE, D. 2011 Multiple scaling in the ultimate regime of thermal convection. *Phys. Fluids* **23**, 045108.

HE, X., BODENSCHATZ, E. & AHLERS, G. 2016 Azimuthal diffusion of the large-scale-circulation plane, and absence of significant non-Boussinesq effects, in turbulent convection near the ultimate-state transition. *J. Fluid Mech.* **791**, R3.

HE, X., FUNFSCHILLING, D., BODENSCHATZ, E. & AHLERS, G. 2012 Heat transport by turbulent Rayleigh–Bénard convection for $Pr \simeq 0.8$ and $4 \times 10^{11} \lesssim Ra \lesssim 2 \times 10^{14}$: ultimate-state transition for aspect ratio $\Gamma = 1.00$. *New J. Phys.* **14**, 063030.

HORN, S. & SHISHKINA, O. 2014 Rotating non-Oberbeck–Boussinesq Rayleigh-Bénard convection in water. *Phys. Fluids* **26**, 055111.

HORN, S., SHISHKINA, O. & WAGNER, C. 2013 On non-Oberbeck–Boussinesq effects in three-dimensional Rayleigh–Bénard convection in glycerol. *J. Fluid Mech.* **724**, 175–202.

HOWARD, L. N. 1966 Convection at high Rayleigh number. In *Applied Mechanics* (ed. H. Görtler), pp. 1109–1115. Springer.

KRAICHNAN, R. 1962 Turbulent thermal convection at arbitrary Prandtl number. *Phys. Fluids* **5**, 1374–1389.

LOHSE, D. & XIA, K.-Q. 2010 Small-scale properties of turbulent Rayleigh–Bénard convection. *Annu. Rev. Fluid Mech.* **42**, 335–364.

MALKUS, M. V. R. 1954 The heat transport and spectrum of thermal turbulence. *Proc. R. Soc. Lond.* A **225**, 196–212.

MANGA, M. & WEERARATNE, D. 1999 Experimental study of non-Boussinesq Rayleigh–Bénard convection at high Rayleigh and Prandtl numbers. *Phys. Fluids* **11** (10), 2969–2976.

NIEMELA, J. J., SKRBEK, L., SREENIVASAN, K. R. & DONNELY, R. J. 2000 Turbulent convection at very high Rayleigh numbers. *Nature* **404**, 837–841.

NIEMELA, J. J. & SREENIVASAN, K. R. 2003 Confined turbulent convection. *J. Fluid Mech.* **481**, 355–384.

OBERBECK, A. 1879 Über die Wärmeleitung der Flüssigkeiten bei Berücksichtigung der Strömungen in Folge von Temperaturdifferenzen. *Ann. Phys. (Berlin)* **243** (6), 271–292.

DU PUITS, R., RESAGK, C. & THESS, A. 2013 Thermal boundary layers in turbulent Rayleigh–Bénard convection at aspect ratios between 1 and 9. *New J. Phys.* **15**, 013040.

DU PUITS, R., RESAGK, C., TILGNER, A., BUSSE, F. H. & THESS, A. 2007 Structure of thermal boundary layers in turbulent Rayleigh–Bénard convection. *J. Fluid Mech.* **572**, 231–254.

ROCHE, P. E., CASTAING, B., CHABAUD, B. & HEBRAL, B. 2004 Heat transfer in turbulent Rayleigh–Bénard convection below the ultimate regime. *J. Low. Temp. Phys.* **134**, 1011–1042.

SCHEEL, J. D., KIM, E. & WHITE, K. R. 2012 Thermal and viscous boundary layers in turbulent Rayleigh–Bénard convection. *J. Fluid Mech.* **711**, 281–305.

SHISHKINA, O., EMRAN, M., GROSSMANN, S. & LOHSE, D. 2017a Scaling relations in large-Prandtl-number natural thermal convection. *Phys. Rev. Fluids* **2**, 103502.

SHISHKINA, O., HORN, S., EMRAN, M. & CHING, E. S. C. 2017b Mean temperature profiles in turbulent thermal convection. *Phys. Rev. Fluids* **2**, 113502.

SHISHKINA, O., HORN, S. & WAGNER, S. 2013 Falkner–Skan boundary layer approximation in Rayleigh–Bénard convection. *J. Fluid Mech.* **730**, 442–463.

SHISHKINA, O., HORN, S., WAGNER, S. & CHING, E. S. C. 2015 Thermal boundary layer equation for turbulent Rayleigh–Bénard convection. *Phys. Rev. Lett.* **114**, 114302.

SHISHKINA, O., WAGNER, S. & HORN, S. 2014 Influence of the angle between the wind and the isothermal surfaces on the boundary layer structures in turbulent thermal convection. *Phys. Rev.* E **89**, 033014.

SHISHKINA, O., WEISS, S. & BODENSCHATZ, E. 2016 Conductive heat flux in measurements of the Nusselt number in turbulent Rayleigh–Bénard convection. *Phys. Rev. Fluids* **1**, 062301(R).

SPIEGEL, E. A. & VERONIS, G. 1960 On the Boussinesq approximation for a compressible fluid. *Astrophys. J.* **131**, 442–447.

STEVENS, R. J. A. M., ZHOU, Q., GROSSMANN, S., VERZICCO, R., XIA, K.-Q. & LOHSE, D. 2012 Thermal boundary layer profiles in turbulent Rayleigh–Bénard convection in a cylindrical sample. *Phys. Rev.* E **85**, 027301.

SUGIYAMA, K., CALZAVARINI, E., GROSSMANN, S. & LOHSE, D. 2007 Non-Oberbeck–Boussinesq effects in two-dimensional Rayleigh–Bénard convection in glycerol. *Europhys. Lett.* **80**, 34002.

SUGIYAMA, K., CALZAVARINI, E., GROSSMANN, S. & LOHSE, D. 2009 Flow organization in two-dimensional non-Oberbeck–Boussinesq Rayleigh–Bénard convection in water. *J. Fluid Mech.* **637**, 105–135.

URBAN, P., HANZELKA, P., MUSILOVA, V., KRALIK, T., MANTIA, M. L., SRNKA, A. & SKRBEK, L. 2014 Heat transfer in cryogenic helium gas by turbulent Rayleigh–Bénard convection in a cylindrical cell of aspect ratio 1. *New J. Phys.* **16**, 053042.

WEI, P. & AHLERS, G. 2014 Logarithmic temperature profiles in the bulk of turbulent Rayleigh–Bénard convection for a Prandtl number of 12.3. *J. Fluid Mech.* **758**, 809–830.

WU, X. Z. & LIBCHABER, A. 1991 Non-Boussinesq effects in free thermal convection. *Phys. Rev.* A **43** (6), 2833–2839.

XIA, K.-Q., LAM, S. & ZHOU, S. Q. 2002 Heat-flux measurement in high-Prandtl-number turbulent Rayleigh–Bénard convection. *Phys. Rev. Lett.* **88**, 064501.

ZHANG, J., CHILDRESS, S. & LIBCHABER, A. 1997 Non-Boussinesq effect: thermal convection with broken symmetry. *Phys. Fluids* **9**, 1034–1042.